Materials Science Forum
ISSN: 1662-9752, Vol. 1156, pp 37-41
doi:10.4028/p-sTgt8T

Submitted: 2024-09-19
Revised: 2025-08-09
Accepted: 2025-08-11
Online: 2025-09-04

New Insights in Orientation and Growth of 150 mm GaN on SiC for HEMT

C. Calabretta[1,a*], N. Piluso[1,b], S. Boninelli[2,c], C. Iatosti [3,d], E. Roy[3e], D. Calabriso[1,f], L. Lilja[4,g], A. Ellison[4,h], C. Riva[4,i], F. Iucolano[1,l] and A. Severino[1,m]

[1]STMicroelectronics, Stradale Primosole 50, 95121 Catania, Italy

[2]CNR-IMM, Strada VIII, 5, 95121 - Catania, Italy

[3]STMicroelectronics, 153 rue des Douets 37100 Tours, France

[4]STMicroelectronics Silicon Carbide AB, Ramshällsvägen 15 SE-602 38 Norrköping, Sweden

[a]cristiano.calabtretta01@st.com, [b]nicolo.piluso@st.com, [c]simona.boninelli@imm.cnr.com, [d]christhophe.iatosti@st.com, [e]emmanuel.roy@st.com, [f]daniele.calabriso@st.com, [g]louise.lilja@st.com, [h]alex.ellison@st.com, [i]carlo.riva@st.com, [l]ferdinando.iucolano@st.com, [m]andrea.severino@st.com

Keywords: GaN, SiC, MOCVD, Photoluminescence, Optical Microscopy.

Abstract. This work explores the application of gallium nitride (GaN)-based solid-state devices for high-power, high-frequency, and high-temperature technologies. It presents an in-depth study of GaN on semi-insulating SiC substrates. The study demonstrates, through bow range investigation, optical microscopy, and X-ray diffraction (XRD), that by adapting growth parameters from those used for Si substrates to those suitable for SiC substrates, it is possible to achieve high-quality crystalline MOCVD growth both under on-axis and 4°off-axis substrate orientations.

Introduction

Recently, gallium nitride (GaN)-based solid-state devices have demonstrated extraordinary effectiveness for high-power, high-frequency, and high-temperature technology. The basic properties of the AlGaN/GaN material combination make it an excellent choice for microwave devices. Silicon is the most cost-effective adopted substrate for large-scale fabrication [1]. However, interfacial stress, dislocation density and melt-back etching caused by Si out-diffusion remain significant disadvantages. GaN on SiC offers superior thermal performance and fewer defects due to better lattice and thermal matching but comes at a higher cost and with manufacturing difficulties. A further challenge is represented by the common use of SiC off-axis substrates. In the off-axis orientation the two orthogonal directions in the vicinal c-plane, along [11-20] and [1-100] (with and without periodic surface steps, respectively) can stimulate anisotropic epitaxy and amplify the effects of the different thermal expansion rates during the cooling process post-growth, potentially causing additional strain and cracking in the GaN layer [2-3].

Materials and Methods

In this work Trimethylgallium (TMGa), Trimethylaluminum (TMAl) and ammonia (NH_3) were used as the precursors for Gallium (Ga), Aluminium (Al) and Nitrogen (N) sources respectively. HEMT layer was carried out on 3 processes where the deposition of a 2 μm GaN buffer layer at 1020 °C was followed by the growth of 16 nm thick AlGaN layer. The epitaxial growth of GaN was conducted employing three distinct methodologies: the Standard Process (SP) method adhered to the established protocol for GaN epitaxy on Si substrates. Subsequently, a specialized procedure was formulated for semi-insulating SiC substrates, which was further bifurcated into two stages,

designated as P1 and P2 on temperature early stage growth parameters. Within the specialized SiC procedure, one of the stages was subjected to trials on SiC substrates measuring 500 µm, both on-axis and 4° off-axis, as well as on a 350 µm SiC substrate. Additionally, a control epitaxial growth on a Silicon substrate was performed to serve as a reference point. The resulting HEMT layer structure AlGaN/GaN were optically characterized by means of flatness analysis, Photoluminescence (PL), Optical microscopy and XRD, to characterize the bow range of wafer as well as PL emission spectra.

Results and Discussion

Upon wafer flatness evaluation, displayed in Fig. 1, distinct behaviors were observed. Adopting the conventional SP process, GaN on SiC wafer exhibited a curvature with a bow range of 187 µm, whereas the Si wafer demonstrated a bow range of 46.2 µm. In the case of on axis SiC substrates, the process variations resulted in flatness values susceptible to thinner SiC substrate thicknesses due to augmented thermal stress during cooling rate, ranging from 78.3 µm to 178.2 µm in P1 and from 37.22 µm to 136.1 µm in P2 when transitioning from a 500 µm to a 350 µm SiC substrate. Among all processes, it is worth noting that off-axis oriented GaN on SiC growths resulted in the lowest bow range as high as 19.75 µm in the P1 and 29.65 µm in the revised process P2. GaN on Si range was, instead, increased in both processes to 136.8 µm and 108.9 µm.

Full Automated Optical microscopy inspection of the wafers revealed a high percentage of Total Usable Area (TUA). Particularly in Fig. 2a, the inspections indicated that the highest 1mm^2 TUA was 99.57% in P2 with 0.46 cm^{-2} defects density. It is noted that the surface remains smooth in the case of GaN on SiC (Fig. 2b), while, in the case of GaN on Si, onset of microcracking is disclosed as the stress can no longer be accommodated elastically, leading to plastic deformation and the generation of slip line and cracks as exhibited in Fig 2c. Full wafer PL analysis, performed with a λ=266 nm excitation laser, revealed that the off-axis GaN on SiC underwent P2 growth exhibited a standard deviation in the GaN signal intensity of 9.9% in band edge spectral region.

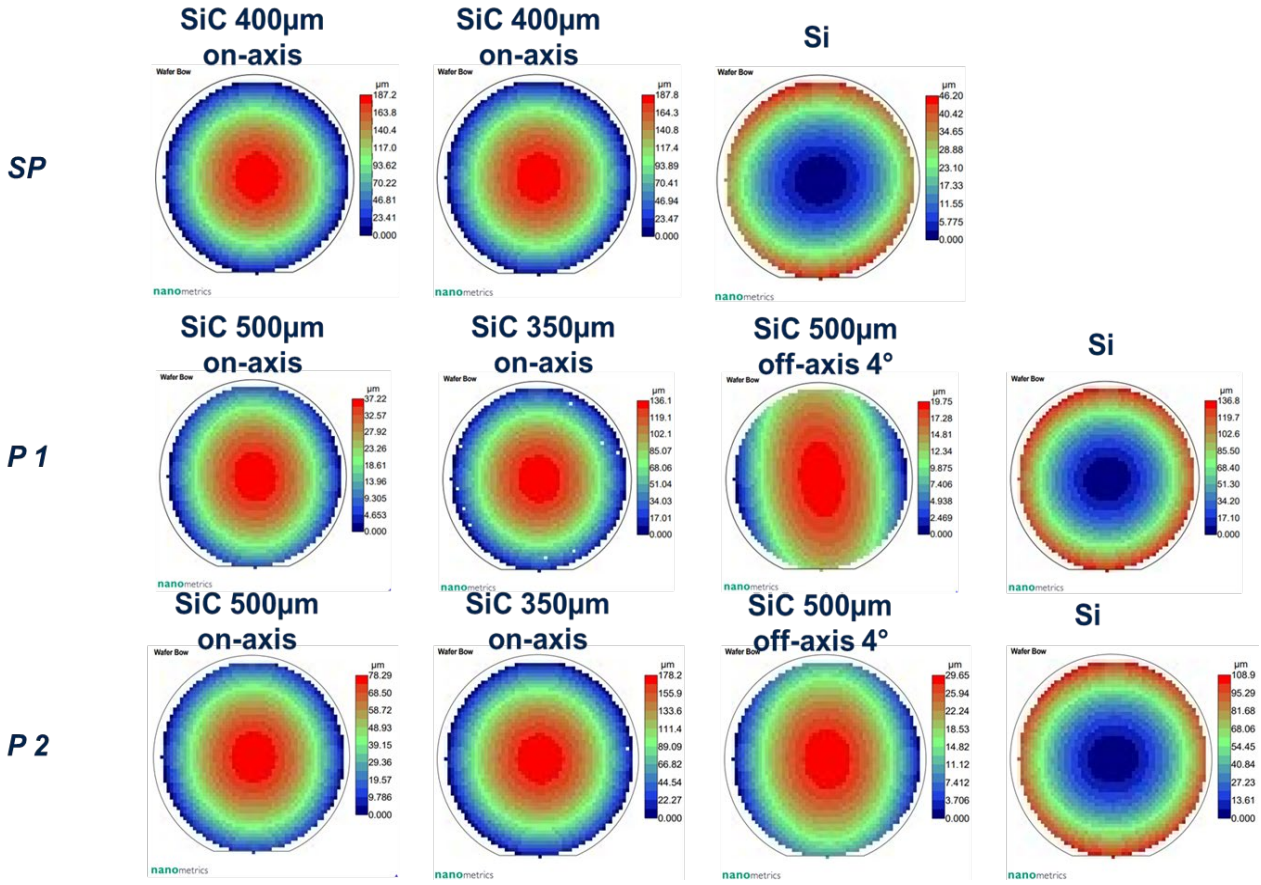

Fig. 1 a) Bow maps for 150 mm GaN on SiC and GaN on Si grown under SP, P1 and P2 processes.

As depicted in Fig. 3a, the spatial map of the emission wavelength indicates a localized bandgap emission peak at (364.1±0.1) nm. As attested for GaN grown under P2 in the PL reported spectra, the emission intensities exhibit variations that rely on crystallographic orientation. Peak intensities are demonstrably higher for the on-axis GaN on SiC sample compared to the off-axis sample, suggesting that the misorientation in the off-axis sample may intensify lattice mismatch and consequently increase the concentration of dislocations. As a result, the off-axis sample manifested a reduced PL intensity. Conversely, for the off-axis, it was attested the rising in PL signal in the intrabandgap region in Fig. 3b. The emission map delineates a specific area indicative of intrabandgap recombination from 500 to 650 nm. This spectral region corresponds to the commonly observed yellow luminescence (YL) band associated with defects in GaN. Potential origins of the YL band in GaN include dislocations as well as various point defects such as Ga vacancies (V_{Ga}) or V_{Ga} complexes, such as $V_{Ga}O_N$ or $V_{Ga}SiN$ and C related point defects [4-6]. The uniformity of this signal across the wafer is quantified by a standard deviation of 6.5%, with a marginal intensification noted towards the periphery of the wafer. Concurrently, the presence of Fabry-Perot oscillations indicates that uniformity in the arrangement of the grown layers is preserved.

The analyses along the XRD (002) axis revealed that the on-axis samples exhibited rocking curves of 266.04 arcseconds and 281.16 arcseconds for the P1 and P2 processes, respectively. In contrast, the off-axis samples showed variations of 331.92 arcseconds and 333.36 arcseconds. These values are competitive with the parameters found for both on axis and off axis configuration within literature [7-10].

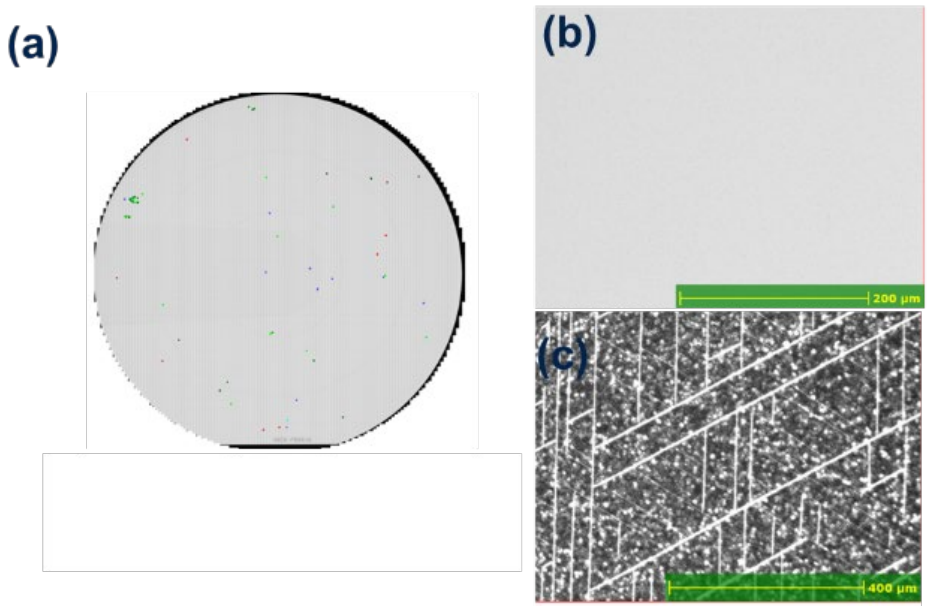

Fig. 2 a) optical microscopy map and image b) for 4° off-axis GaN on SiC grown under P2 and an image.

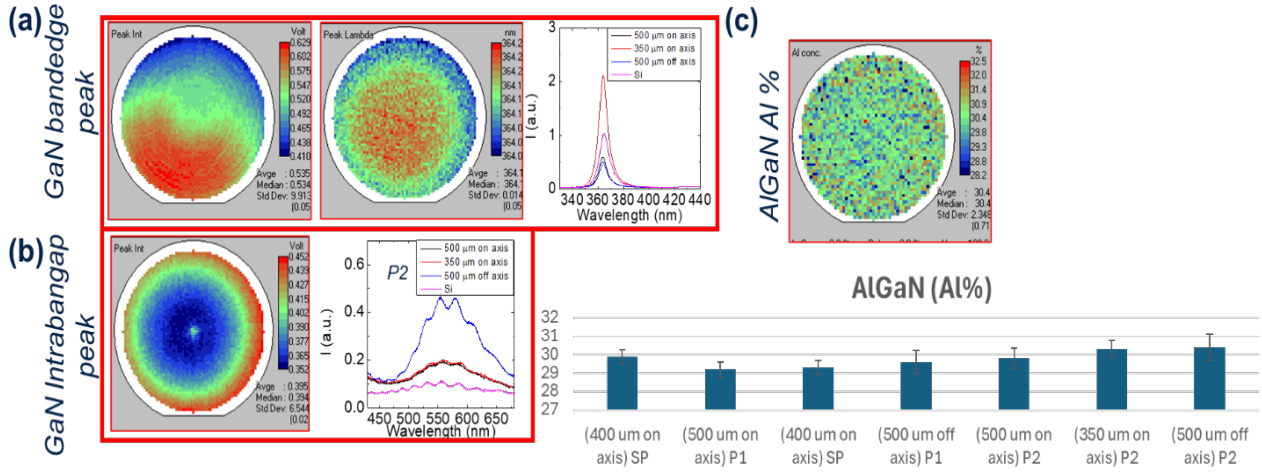

Fig. 3 a) of GaN on Si under P2; b) Intensity and wavelength PL maps over band edge for 4° off-axis GaN on SiC grown under P2 with band edge related spectra of wafers grown under P2. b) Intrabandgap map for 4° off-axis GaN on SiC grown under P2 and related spectra for wafer grown under P2; c) Al fraction map for for 4° off-axis GaN on SiC grown under P2 and values for other wafers.

The compositional analysis depicted in Fig. 3c illustrates that the off-axis sample from process P2 contains the Al fraction of (30.4±0.71)%. This data suggests that the P2 facilitates a higher Al incorporation rate, and exhibit an upward trend in the Al fraction from process P1 to process P2. In light of the results, the research presented herein provides valuable insights into the optimization of 150 mm GaN on SiC MOCVD growth, establishing the 4° off-axis SiC substrate as a promising contender for the improvement of GaN on SiC High Electron Mobility Transistors (HEMTs).

Summary

Within this work, High Electron Mobility Transistor (HEMT) layer deposition involved three processes, starting with a 2 µm GaN buffer layer at 1020 °C, followed by a 16 nm thick AlGaN layer. GaN epitaxial growth was conducted using three methodologies: the Standard Process (SP) for GaN on Si substrates, and two specialized procedures (P1 and P2) for semi-insulating SiC substrates, differing in early thermal process ramps. Trials were conducted on 500 µm and 350 µm SiC substrates, both on-axis and 4° off-axis, with a control growth on a Silicon substrate for reference. Wafer flatness evaluations revealed distinct behaviors: GaN on SiC exhibited a bow range of 187 µm, while GaN on Si showed 46.2 µm. Process variations affected flatness, especially in thinner SiC substrates due to thermal stress. Off-axis GaN on SiC showed the lowest bow ranges (19.75 µm in P1 and 29.65 µm in P2). Optical microscopy indicated high TUA, with P2 achieving 99.57% TUA (grid 1x1mm) and 0.46 cm^{-2} defect density. GaN on SiC surfaces remained smooth, while GaN on Si exhibited microcracking. PL analysis revealed a standard deviation of 9.9% in GaN signal intensity for off-axis GaN on SiC under P2. Emission intensities varied with crystallographic orientation, with higher intensities in on-axis samples. The emission map indicated intrabandgap recombination, associated with defects, and a standard deviation of 6.5% in signal uniformity. XRD analysis showed rocking curves of 266.04 arcseconds and 281.16 arcseconds for on-axis samples (P1 and P2), and 331.92 arcseconds and 333.36 arcseconds for off-axis samples. Compositional analysis indicated higher Al incorporation in P2, with an Al fraction of (30.4±0.71)%. These findings provide valuable insights into optimizing 150 mm GaN on SiC MOCVD growth, highlighting the potential of 4° off-axis SiC substrates for improving GaN on SiC HEMTs.

References

[1] Cai, Yuefei, et al. "Strain analysis of GaN HEMTs on (111) silicon with two transitional AlxGa1− xN layers." Materials 11.10, 1968, (2018)

[2] Yao, Lei, et al. "An Inductive Coupling Based CMOS Wireless Powering Link for Implantable Biomedical Applications." International Journal of Electronics and Communication Engineering 6.9 (2012): 931-934

[3] Drechsel, P., and H. Riechert. "Strain controlled growth of crack-free GaN with low defect density on silicon (1 1 1) substrate." Journal of crystal growth 315.1, 211-215, (2011).

[4] Reshchikov, Michael A., and Hadis Morkoç. "Luminescence properties of defects in GaN." *Journal of applied physics* (2005), 97.6.

[5] Calabretta, Cristiano, et al. "GaN Cap UV Spectroscopy Assessment in AlGaN/GaN HEMT." *Solid State Phenomena* 36, 27-31, (2024).

[6] Scandurra, Antonino, et al. "Two-dimensional electron gas isolation mechanism in Al0. 2Ga0. 8N/GaN heterostructure by low-energy Ar, C, Fe ion implantation." *Applied Surface Science* 674 (2024): 160885.

[7] Su, Chung-Wang, et al. Solid-State Electronics 179,107980, (2021).

[8] Feng, Sirui, et al. "Strain Release in GaN Epitaxy on 4° Off-Axis 4H-SiC." *Advanced Materials* 34.23, 2201169, (2022).

[9] Cho, E., et al. "Impact of AlN nucleation layer on strain in GaN grown on 4H-SiC substrates." *Journal of crystal growth* 371, 45-49, (2013).

[10] Susanto, Iwan, Ken-Yuan Kan, and Song Yu. "Temperature effects for GaN films grown on 4H-SiC substrate with 4° miscutting orientation by plasma-assisted molecular beam epitaxy." *Journal of Alloys and Compounds* 723 (2017): 21-29.